Structural properties of amorphous hydrogenated carbon. II. An inelastic neutron-scattering study

P. J. R. Honeybone, R. J. Newport, and J. K. Walters
Physics Laboratory, The University, Canterbury, Kent, CT2 7NR, United Kingdom

W. S. Howells and J. Tomkinson
Neutron Division, Rutherford Appleton Laboratory, Didcot, OX11 0QX, United Kingdom
(Received 27 September 1993)

Inelastic-neutron-scattering experiments have been performed on samples of amorphous hydrogenated carbon, prepared from acetylene and propane, containing about 35 and 32 at. % hydrogen, respectively. In these hard carbons, the hydrogen is predominantly bonded to sp^3 carbon, with approximately equal concentrations of CH and CH_2 groups. There is little hydrogen in other bonding environments, and a small amount of H_2 is trapped in cages in the material.

INTRODUCTION

Amorphous hydrogenated carbon may be prepared harder, denser, and more resistant to chemical attack than any other solid hydrocarbon. This, coupled with infrared transparence over a wide energy range and controllable optical gap and refractive index have led to a wide range of potential applications.[1,2] These properties are reviewed elsewhere, along with current structural models.[3,4]

Neutron-diffraction results presented in paper I of this series, see also Refs. 5 and 6, lead to a good understanding of the amorphous network giving rise to the static structural properties of amorphous hydrogenated carbon. Little information, however, is provided on the hydrogen bonding environment, besides showing that most hydrogen is bonded to carbon and that some CH_2 groups exist. Inelastic neutron scattering has the potential to determine quantitatively the dominant hydrogen bonding environments through a study of the characteristic vibrational frequencies.

The most commonly used technique for determining the hydrogen bonding environment is infrared spectroscopy (e.g., Refs. 7–9), which also uses the characteristic vibrations of the CH_n groups to determine which are present. The high-resolution of infrared spectroscopy has enabled an assignment of all possible *a*-C:H vibrational modes.[7] Most work (e.g., Refs. 7 and 9) uses the areas obtained from a multiple Gaussian fit to the C-H stretch bands to estimate the concentrations of CH_n groups, although Vandentop *et al.*[8] have used CH_2 and CH_3 bending vibrations to form an estimate of the sp^3 CH_2:CH_3 ratio.

The problem with this approach is the dependence of the absorption intensity on a change in dipole moment with vibrational excitation. This matrix element can only be estimated from similar materials and may be liable to change as the underlying amorphous network changes. So, although using absorption coefficients from samples of known bonding environments can lead to estimates of the relative concentrations of the hydrogen groups, these are liable to be inexact.

Inelastic neutron scattering, however, does not suffer from this problem as the observed scattering intensity is directly related to the eigenvector of the vibration, although energy resolution is not as good. The TFXA spectrometer at the ISIS pulsed neutron source (Rutherford Appleton Laboratory, UK) is well suited to determining the vibrational density of states of hydrogenated material, as it is optimized for energy resolution, albeit with a resultant loss in Q resolution.[10] The MARI spectrometer, on the other hand enables the Q dependence of the vibrational frequencies to be studied, and so provides complementary information to that obtained on TFXA.[10]

A combination of the two spectroscopic methods (infrared frequencies and INS intensities) enables the relative concentrations of the dominant hydrogen bonding configurations to be determined.

EXPERIMENTAL DETAILS

Two samples of amorphous hydrogenated carbon were prepared using a saddle-field ion-beam source.[11] They were deposited onto copper substrates from acetylene and propane precursor gases, respectively, (as *a*-C:H does not adhere to copper, this proved an excellent means of producing the large powder samples required for neutron-scattering experiments).

The inelastic neutron-scattering data were collected on the TFXA and MARI spectrometers at the ISIS spallation neutron source, Rutherford Appleton Laboratory.[10] (The TFXA spectrometer generates high-intensity data integrated over momentum transfer, $\hbar Q$, whereas the data from MARI offers a relatively high degree of Q resolution.) Complementary infrared measurements were performed using a Perkin-Elmer dual beam instrument, for which the powder samples were diluted with potassium bromide (which is infrared transparent) and pressed into pellets.

The density measurements were performed using a residual volume technique and the compositions were determined using a Carlo-Erba CHN combustion analyzer. These results are summarized in Table I. Note

TABLE I. The precursor gas and resultant *a*-C:H film compositions and the film densities.

	Precursor gas	C:H ratio in gas	C in film (at. %)	H in film (at. %)	Density g cm^{-3}	Number density (atoms Å^{-3})
Sample 1	Acetylene	1:1	65	35	1.8	0.134
Sample 2	Propane	3:13	68	32	2.0	0.140

that the values given for the film densities assume a ~10% void content.

DATA CORRECTION AND ANALYSIS

TFXA data: Incoherent inelastic neutron scattering

In the incoherent approximation,[12] the scattering function can be directly related to the vibrational density of states, $g(\omega)$:

$$S^s(Q,\omega)=\frac{\hbar Q^2}{2m}e^{-2W}\frac{(1+\langle n_\lambda\rangle)}{\omega}g(\omega)\,, \tag{1}$$

where $S^s(Q,\omega)$ is the self-scattering, $\hbar Q$ is the momentum transfer, $\hbar\omega$ the energy transfer, $\langle n_\lambda\rangle$ is the population factor for mode of frequency ω_λ and e^{-2W} is the Debye-Waller factor. A more complete account of the theory is given elsewhere.[12,13]

In an amorphous system, such as *a*-C:H, there are many possible bonding environments, which give rise to vibrations at many different frequencies. Hydrogen has a much larger incoherent scattering cross section than carbon so that in the incoherent approximation, the resultant can all be ascribed to vibrations involving hydrogen motion. Due to its light mass, hydrogen vibrations are generally of a higher frequency than those of the network (i.e., they are not degenerate with network vibrations), allowing a fully separate treatment. A further simplification is provided by the univalence of hydrogen, which restricts the number of local bonding environments that need to be considered.

The CLIMAX program[14] produces a least-squares fit of a model inelastic spectrum, calculated for a user-defined "molecule," to the observed inelastic neutron scattering, based on the eigenvectors of the characteristic vibrational frequencies. Tomkinson[13] and Gans[15] provide an excellent introduction to the inelastic neutron-scattering theory and vibrational spectroscopy, upon which this program is based.

In modeling an amorphous hydrogenated system, small "molecules" or structural units are created, which are capable of representing all the vibrational modes of each hydrogenated group (e.g., CH, CH_2, etc.). For simplicity, each molecule was kept as small as possible. Within each molecule, vibrations are constructed from a set of internal coordinates (bond stretches, bends, etc.), each of which is assigned a force constant. These force constants are fitted to the infrared frequencies and then to the inelastic neutron-scattering spectrum, with appropriate weightings being provided via this process for each "molecule." This weighting indicates the fraction of hydrogen in each of the model hydrogenated groups.

MARI data: Q resolved

The chopper on MARI selects the incident neutron energy, which allows the final energy and momentum transfer to be simultaneously measured, albeit with a loss of intensity (relative to other instruments such as TFXA). Once corrections for attenuation, multiple scattering, and attenuation have been applied, the dynamical structure factor, $S(Q,\omega)$, is obtained. A more detailed account of the data analysis procedure can be found elsewhere.[16] Integration over Q or ω ranges allows vibrational densities of states or Debye-Waller factors to be estimated.

RESULTS AND DISCUSSION

TFXA data: CLIMAX—models and frequency assignments

The inelastic neutron scattering spectra of the *a*-C:H samples can be split into two regions—a low-frequency region (<500 cm^{-1}) which is dominated by the scattering from residual quantities of the liquid nitrogen used to quench the samples and a high-frequency region (>500 cm^{-1}) consisting of localized CH_n stretch and bend vibrations (see Fig. 1).

The low-frequency region of the inelastic neutron-scattering spectra of both samples are very similar to that of nitrogen indicating little contribution from *a*-C:H in

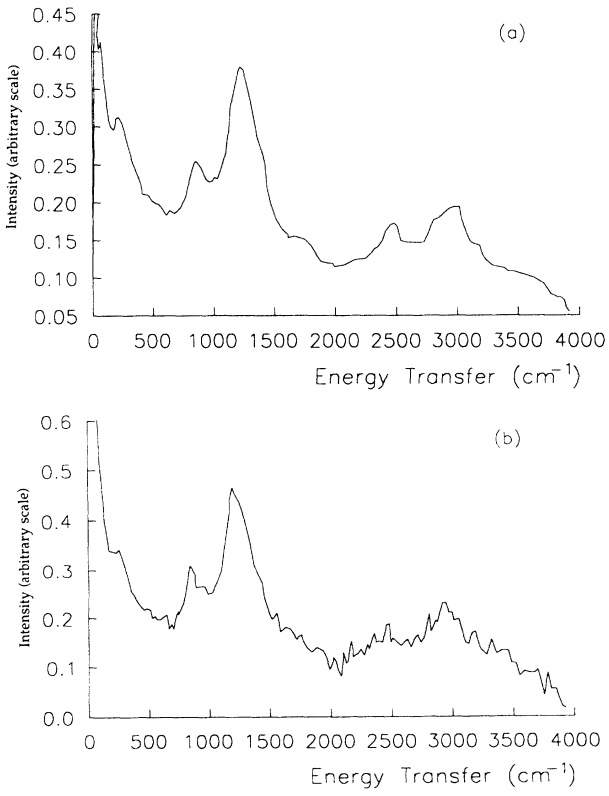

FIG. 1. Inelastic neutron scattering of *a*-C:H prepared from (a) acetylene (sample 1) and (b) propane (sample 2) obtained on the TFXA spectrometer.

this region. There is, however, likely to be an additional contribution from molecular hydrogen, which is obscured by the nitrogen scattering.[17] Unfortunately, comparison with infrared and Raman spectroscopy is not possible as these vibrations occur below the minimum energies reported by these techniques (e.g., Refs. 18 and 19).

Between 700 and 1500 cm^{-1} are the CH_n bending vibrations, which will be dealt with in the following sections. The CH_n stretch band and overtone of the CH_n bending vibrations occur at 3000 and 2500 cm^{-1}, respectively. Unfortunately, the resolution in this region is low and, hence, no difference can be seen between the samples.

The inelastic neutron-scattering spectra of the high-frequency region of the *a*-C:H samples are very similar to each other which implies similarities in the hydrogen distributions.

As hydrogen is univalent, it is necessarily connected to the network by only one bond. This limits the number of possible hydrogen bonding environments to sp^3 CH, CH_2, and CH_3 groups, sp^2 olefinic and aromatic CH and olefinic CH_2 and *sp* CH. The incoherent neutron-scattering cross section of hydrogen is much higher than that of carbon, which means the inelastic neutron-scattering spectrum will be dominated by scattering from hydrogen. Additionally, the low mass of hydrogen results in C-H vibrations being of generally higher frequency than carbon backbone vibrations. Hence these vibrations are independent from those of the carbon network, enabling analysis of the hydrogen vibrational modes separate from those of the network. (The Raman modes associated with sp^2 carbon at 1400 and 1530 cm^{-1} and those estimated for sp^3 carbon[19] are not seen in the inelastic neutron-scattering spectra.)

The dominant peaks are at 875 and 1280 cm^{-1}, with additional component bands visible as shoulders either side of the 1280-cm^{-1} peak. Comparison of these peaks with Dischler's IR assignments[7] shows one possible combination is the sp^2 CH *in-plane* (1280 cm^{-1}) and *out-of-plane* (840 cm^{-1}) bending vibrations. This, however, cannot be the case, as the out-of-plane mode of this group would be expected to be more intense than the in-plane mode—contrary to experiment.

Since earlier NMR (Ref. 20) and infrared spectroscopy[7] have suggested that hydrogen is predominantly bonded to sp^3 carbon, consideration should be given to the vibrational modes of the sp^3 CH_n groups. Further, infrared spectroscopy by Vandentop *et al.*[8] has shown the sp^3 CH_3:CH_2 ratio in *a*-C:H to be very small. This limits initial consideration to sp^3 CH and CH_2 groups.

According to Dischler,[7] the CH group would give rise to a C-H bending vibration at 1370 cm^{-1} and C-C and C-H stretching vibrations at 885 and 2920 cm^{-1}, respectively. The CH_2 group would give rise to a bending vibration at 1440 cm^{-1}, a twist at 1170 cm^{-1}, a wag at 1030 cm^{-1} and a rock at 700 cm^{-1} as well as C-C and C-H stretch vibrations.

Models based on these assignments failed to produce a good fit to the observed inelastic neutron-scattering spectrum. In particular, the theoretical intensity at 700 cm^{-1} is too large and only a poor fit could be obtained to the 1280-cm^{-1} peak.

Comparison with the vibrational modes of SiH and SiH_2 groups in amorphous hydrogenated silicon[21] reveals further problems with the bending assignments of Dischler and others. Although the carbon and silicon masses and C-H and Si-H bond strengths are different, the site symmetry is the same, so whilst the vibrational frequencies will differ between CH_n and SiH_n groups, the ordering of modes in ascending vibrational frequency would be expected to be the same. Table II compares the CH and CH_2 bending assignments of Dischler[7] with SiH and SiH_2 assignments of Cardona.[21]

In making his assignments, Dischler used published data[22,23] on organic molecules. In cases of disagreement between the sources, a "best guess" had to be made for the particular assignment.[24] Significant differences occur between the assignments of Dischler[7] and Dollish, Fately, and Bentley[22] in the frequency of the CH bend and three of the CH_2 torsional vibrations (see Table III).

If the CH and CH_2 bending vibrations are assigned in accordance with those of Dollish, Fately, and Bentley,[22] a good fit to the experimental data (see Fig. 2) is obtained. The frequencies used for the best fit can be seen in Table III and are in accordance with what might be expected from *a*-Si:H.[21] Robertson has recently compiled an updated list of vibrational frequencies and assignments for CH_n groups;[4] these new assignments are in agreement with those used here.

Modeling with sp^3 CH and CH_2 groups alone shows acceptable agreement with experiment. Further refinement, by using *small* quantities of sp^2 CH_n and sp^3 CH_3 (less likely) groups may provide some improvement to the overall fit to the data, but the hydrogen present in these two environments is likely to be less than 20% of the total hydrogen content.

Having established that the observed inelastic neutron-scattering spectrum can be explained to a reasonable approximation in terms of a combination of sp^3 CH and CH_2 groups, the next step is to estimate the relative quantities of the two groups. The results obtained for the best fit to the experimental data (see Fig. 2) are given in Table IV.

The experimental results show that there are at least as many CH_2 groups as CH groups in both samples, contrary to what would be expected from a random distribution of hydrogen amongst carbon sites, and from the analysis of the infrared C-H stretch vibration[7,25] which suggest that CH sites would dominate. It should be not-

TABLE II. Bending vibrations of CH, CH_3, SiH, and SiH_2 groups.

Assignment	Frequency (Ref. 7)	Assignment	Frequency (Ref. 21)
CH_2 rock	700 cm^{-1}	SiH_2 rock	395 cm^{-1}
CH_2 wag	1030 cm^{-1}	SiH_2 wag	685 cm^{-1}
CH_2 twist	1170 cm^{-1}	SiH_2 twist	685 cm^{-1}
CH bend	1370 cm^{-1}	SiH bend	685 cm^{-1}
CH_2 bend	1440 cm^{-1}	SiH_2 bend	885 cm^{-1}

TABLE III. Comparison of the CH and CH_2 bending vibrations from Refs. 7, 22, and those used in this work.

Vibration	Dischler (Ref. 7)	Dollis *et al.* (Ref. 22)	This work
C-C stretch	885 cm^{-1}	1132–885 cm^{-1}	875 cm^{-1}
CH_2 rock	700 cm^{-1}	1060–719 cm^{-1}	1030 cm^{-1}
CH bend	1370 cm^{-1}	1160 cm^{-1}	1190 cm^{-1}
CH_2 twist	1170 cm^{-1}	1310–1175 cm^{-1}	1300 cm^{-1}
CH_2 wag	1030 cm^{-1}	1411–1174 cm^{-1}	1330 cm^{-1}
CH_2 bend	1440 cm^{-1}	1473–1446 cm^{-1}	1470 cm^{-1}

ed, however, that the most recent infrared studies,[25] with a $CH:CH_2$ ratio of 1.5:1 actually implies more hydrogen in CH_2 groups than in CH groups.

The $CH:CH_2$ ratio being greater for sample 1, than for sample 2 would be expected with increasing hydrogen concentration. The correspondence of the $CH:CH_2$ ratio with the number density is perhaps significant. It could indicate that the inclusion of CH_2 groups results in small void regions in the structure, thus reducing the overall density. Certainly, the two hydrogen atoms in a CH_2 group would form a region across which the network could not be connected. This conclusion can only be drawn cautiously, however, on the basis of this data alone. The NMR data presented in paper III provide much more specific information on this question.

Further information can be gained by a comparison of the degree of hydrogenation with the carbon content of

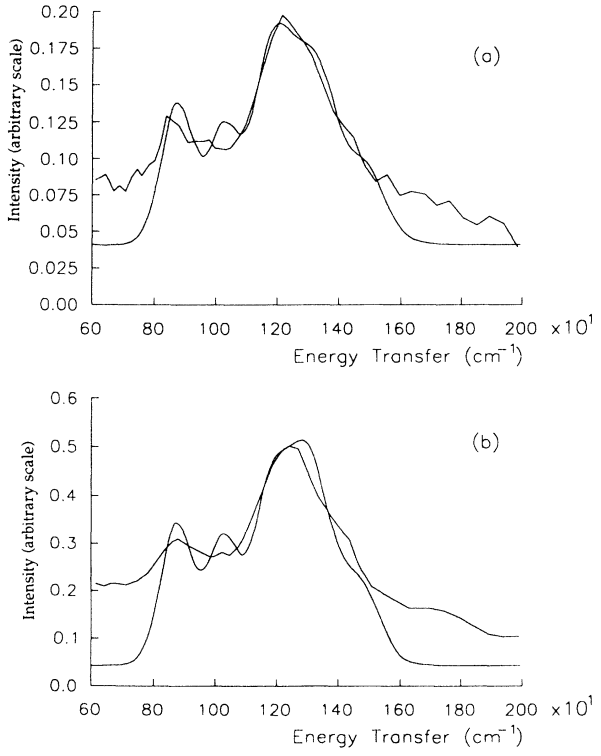

FIG. 2. Inelastic neutron-scattering spectrum of *a*-C:H prepared from (a) acetylene and (b) propane. The high-frequency region and fits obtained using the CLIMAX program.

TABLE IV. Comparison of hydrogen content with $CH:CH_2$ ratio for *a*-C:H produced from acetylene (sample 1) and propane (sample 2).

	Hydrogen content (at. %)	$CH:CH_2$ Ratio	Total number density (atoms $Å^{-3}$)
Sample 1	35	0.8	0.134
Sample 2	32	1.0	0.140

the films and comparing with information from neutron-diffraction data (see paper I). This allows a more complete picture of the carbon local bonding to be obtained (see Table V).

It is interesting to note that the fraction of carbon present in sp^3 CH groups does not change between the samples, even though there is a change in the total hydrogen content. It seems that the only change is in the CH_2 content, which is linked to a polymeric phase (chains of CH_2 groups). Further neutron work is required to investigate this in more detail, but again the NMR data in paper III of this series allows us to be rather more specific.

A summation of the sp^3 CH and CH_2 fractions agree, to within experimental uncertainties, with the sp^3 content obtained from neutron-diffraction data (see paper I). This implies that there are relatively small amounts of unhydrogenated sp^3 C/CH_3 groups, and suggests that quaternary carbon (a carbon bonded to four other carbon atoms), the most rigidly bonded arrangement known for carbon, may make little overall contribution to the network properties of *a*-C:H, including hardness [as is assumed by current models (e.g., in Ref. 26)]. Also, the trade-off between CH_2 sites (at high hydrogen content) and clustered sp^2 sites (at low hydrogen content), neither of which contribute to network rigidity, cannot explain the observed maximum hardness for intermediate hydrogen contents, as Table V shows a greater increase in sp^2 concentration than the drop in CH_2 concentration as the hydrogen content falls.

The dominant carbon bonding environment is sp^2 hybridized (see paper I) even at the highest hydrogen content, of which olefinic carbon makes the largest contribution. The carbon-carbon double bond associated with an olefinic pair is resistant to rotation (unlike a carbon-carbon single bond), thus adding extra rigidity. In a pure sp^2 carbon (e.g., graphite), this would not normally result in a hard material, as the bonds are all in one plane, allowing delocalization of the π electrons throughout the interconnecting network; there are no interplanar bonds, resulting in a soft material. Tamor and Hass have, how-

TABLE V. Comparison of the carbon content with proportions of dominant hydrogen bonding environments for *a*-C:H prepared from (a) acetylene (sample 1) and (b) propane (sample 2).

	Carbon content	sp^3 CH	sp^3 CH_2	Other CH_n
Sample 1	0.65	0.08–0.10	0.10–0.13	0–0.05
Sample 2	0.68	0.08–0.10	0.09–0.11	0–0.05

ever, proposed a superhard three-dimensional sp^2 carbon,[27] which may help our understanding of hard a-C:H. This is achieved by allowing rotation about the single bonds, so that, although all bond angles are 120° and near neighbors are in a plane, dihedral angles are 60°. This results in a very hard network (their calculations suggest a hardness greater than that in diamond).

In modeling the hardness of a-C:H,[26] Robertson agrees that olefinic carbon would contribute to network rigidity, but then ignores it on the grounds of very low concentration. Thus, by assuming that all sp^2 carbon is in aromatic or graphitic clusters, he obtains good agreement between his theoretical hardness calculations and experimental measurements for all but the lowest sp^2 content a-C:H films.

This is in stark contrast to the films studied here, where most carbon is sp^2 hybridized and yet there is both high olefinic content and hardness. The implication of this is that the olefinic carbon is responsible for the high hardness in these films. The hydrogen would seem to be important more as an inhibitor of aromatic clustering than as a means of increasing the sp^3 "diamondlike" carbon as suggested by current models.[3,28,29]

MARI data

The $S(Q,\omega)$ for samples 1, obtained on the MARI spectrometer is shown in Fig. 3. There are two recoil lines corresponding to the motion of hydrogen and carbon atoms after collision with the neutron. The gradient of the recoil line is characteristic of the nuclear mass,[16] and identifies the steeper line as hydrogen and the shallower as carbon.

From the contour map, it is possible to see maxima superimposed on the recoil lines at three energies—0 meV

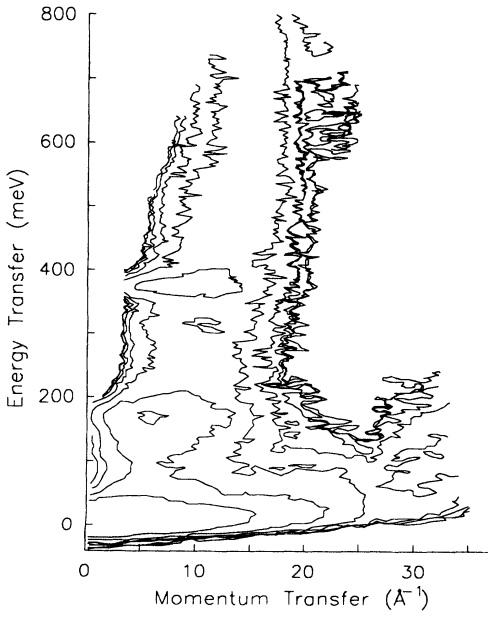

FIG. 3. Contour map of $S(Q,\omega)$ for sample 1 (prepared from acetylene). Data collected on the MARI spectrometer using 800-meV incident neutrons.

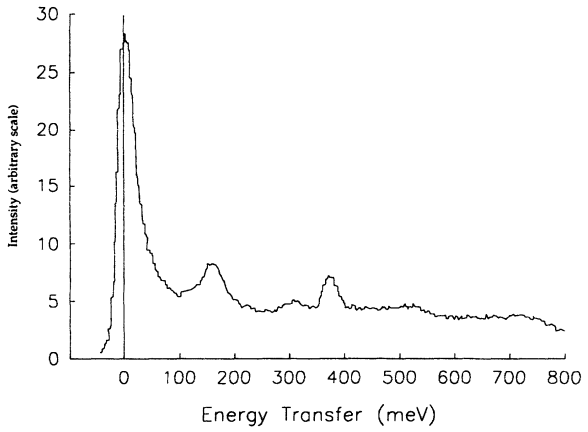

FIG. 4. Inelastic neutron-scattering spectra for sample 1 (prepared from acetylene) showing the C-H stretch (375 meV), bend (150 meV), and the overtone of the C-H bend (300 meV). Data collected on the MARI spectrometer using 800-meV incident neutrons.

(the elastic line), 160 meV or 1280 cm^{-1} (the CH_n bending vibrations) and 375 meV or 3000 cm^{-1} (the CH_n stretching vibrations). It is interesting to note the intensity in these latter peaks extends outside the hydrogen recoil line, indicating an effective mass greater than that of hydrogen (i.e., a carbon contribution to the effective mass).

Integrating this contour map over momentum transfer generates a vibrational density of states similar to that found on TFXA, which show these and other features more clearly (see Fig. 4).

The carbon-carbon stretch seen in the TFXA data is revealed as a shoulder to the CH_n bending vibration at 110 meV (890 cm^{-1}) and the first overtone of the CH_n bending vibration occurs at 310 meV (2500 cm^{-1}). Another peak appears at 520 meV and is discussed in more detail below.

Small quantities of molecular hydrogen have already been shown to be trapped in a-C:H in high-pressure spheroidal cages in our earlier work.[17] The effective hy-

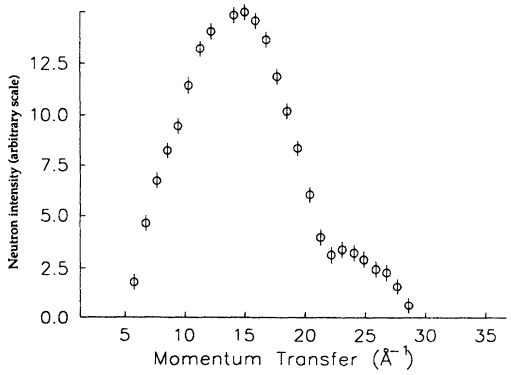

FIG. 5. Debye-Waller factor for the recoil scattering between 465 and 571 meV of a-C:H prepared from acetylene (sample 1). Data collected on the MARI spectrometer using 800-meV incident neutrons.

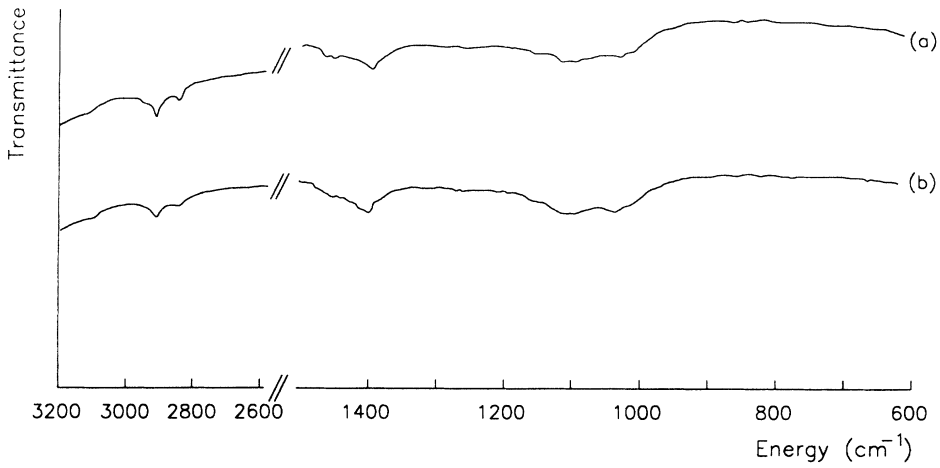

FIG. 6. The infrared spectra for prepared from (a) acetylene (sample 1) and (b) propane (sample 2).

drostatic pressure, estimated from compressive stress measurements on the basis of measured substrate bending is >2 GPa, which is consistent with other work.[30] This compares with a pressure of 0.2–0.4 GPa for hydrogen in *a*-Si:H based on Chabal and Patel's infrared data.[31]

The inelastic neutron-scattering data from MARI could hold further evidence for molecular hydrogen in *a*-C:H since the 520-meV peak (see Fig. 4) is in close proximity to the H-H stretch vibration [541 meV (Ref. 23)].[32] Unfortunately, the combination for the CH_n stretch and bend vibrations is expected to give intensity in this region and, hence, definitive assignment is not yet possible. This is because the Debye-Waller factors of the vibrational modes are obtained by integrating the $S(Q,\omega)$ at constant Q across each vibrational peak. The pre-exponential part of the Debye-Waller factor should be proportional to Q^2 for a fundamental and Q^4 for a combination or overtone. In practice a complication occurs due to the recoil lines, which also have a Q^4 dependence (see Fig. 5) and dominate over the weaker vibrational modes. This limits the usefulness of this technique until the recoil scattering can be calculated using molecular-dynamics simulation. It is, however, possible to confirm the fundamental characteristics of the CH_n 160 meV (1280 cm^{-1}) bend and 375 meV (3000 cm^{-1}) stretch vibrations.

Infrared spectroscopy

The conclusion drawn from the TFXA data that the hydrogen is bonded preferentially in sp^3 CH and CH_2 groups, with little difference between the samples, is supported by our infrared measurements (see Fig. 6).

There are two peaks in the C-H stretch band, at 2920 cm^{-1} (the expected frequency of the CH and CH_2 asymmetric stretches[7] and at 2850 cm^{-1} (the CH_2 symmetric stretch). The absence of other features suggests strongly (though qualitatively only) that other carbon bonding environments are low in concentration.

The CH_n bending vibrations in the 1000–1500 cm^{-1} region shows two broad peaks at 1030 and 1130 cm^{-1} which correspond to the CH_2 rock and CH bend. It is not clear if a sharp peak at 1400 cm^{-1} is the CH_2 wag or bend or a carbon network vibration analogous to the 1400-cm^{-1} mode seen in Raman spectroscopy[19] (the CH_2 twist is infrared inactive). These peak positions are in general agreement with the assignments based on the inelastic neutron scattering presented above.

Water absorbed by the potassium bromide produces broad features between 1500 and 1800 cm^{-1} and between 3000 and 3700 cm^{-1}, corresponding to the bend and stretch vibration-rotation modes. Fortunately, these do not obscure any of the CH_n vibrations, and only produce a small background slope to the CH_n stretch vibrations.

CONCLUSIONS

The incoherent inelastic neutron-scattering data has highlighted problems with the accepted assignments for the CH and CH_2 bending vibrations.[7] New assignments have been used to show that the contributions principal to the high frequency (> 500 cm^{-1}) region of the inelastic neutron-scattering spectrum are from sp^3 CH and CH_2 groups, with at least as many CH_2 as CH groups. This implies that at least $\frac{2}{3}$ of the hydrogen is in the form of CH_2 groups. There seems to be a correlation between increased CH_2 concentrations and decreased network densities, although a wider compositional range of samples needs to be studied to establish the relationship between CH:CH_2 ratio and hydrogen content. Comparison with neutron-diffraction results (see paper I) suggests that there is relatively little unhydrogenated sp^3 carbon in the samples—a question probed in more detail by the NMR work presented in paper III. Small quantities of other hydrogen bonding environments exist, including molecular hydrogen, which is present in a high-pressure environment.

ACKNOWLEDGMENTS

We would like to thank A. Evans, Dr. P. Revell, and Dr. J. Franks of Ion Tech Ltd. for their help in depositing the *a*-C:H, A. Fassam (Chemistry Dept., UKC) for his help in determining compositions and other members of the Kent group, Dr. S. Bennington and Dr. J. Robertson for helpful discussions. P.J.R.H. and J.K.W. acknowledge the SERC for support.

[1]A. H. Lettington, in *Diamond and Diamondlike Films and Coatings,* edited by J. C. Angus, R. E. Clausing, L. L. Horton, and P. Koidl (Plenum, New York, 1991).
[2]S. Aisenberg and F. M. Kimock, Mater. Sci. Forum **52-53**, 1 (1989).
[3]J. C. Angus, P. Koidl, and S. Domitz, in *Plasma Deposited Thin Films,* edited by J. Mort and F. Jansen (CRC, Boca Raton, 1986), Chap. 4, p. 89.
[4]J. Robertson, Prog. Solid State Chem. **21**, 199 (1991).
[5]J. K. Walters, P. J. R. Honeybone, D. W. Huxley, R. J. Newport, and W. S. Howells, J. Phys. Condens. Matter **5**, L387 (1993).
[6]D. W. Huxley, P. J. R. Honeybone, R. J. Newport, W. S. Howells, and J. Franks, in *Novel Forms of Carbon,* edited by C. I. Renschler, J. J. Pouch, and D. M. Cox, MRS Symposia Proceedings No. 270 (Materials Research Society, Pittsburgh, 1992), p. 493.
[7]B. Dischler, in *Amorphous Hydrogenated Carbon Films,* edited by P. Koidl and P. Oelhafen, *Proceedings of the European Materials Research Society* (Les Editions de Physique, Paris, 1987), Vol. 17, p. 189.
[8]G. J. Vandentop, M. Kawasaki, K. Kobayashi, and G. A. Somorjai, J. Vac. Sci. Technol. A **9**, 1157 (1991).
[9]J. C. Angus, J. E. Stultz, P. J. Shiller, J. R. MacDonald, M. J. Mirtich, and S. Domitz, Thin Solid Films **118**, 311 (1984).
[10]*ISIS Experimental Facilities,* edited by B. Boland and S. Whapham (Rutherford Appleton Laboratory, 1992).
[11]J. Franks, Vacuum **34**, 259 (1984).
[12]J. D. Axe, *Physics of Structurally Disordered Materials,* edited by S. S. Mitra (Plenum, New York, 1976), p. 507.
[13]J. Tomkinson, in *Neutron Scattering at a Pulsed Source,* edited by B. D. Rainford, R. J. Newport, and R. Cywinski (Hilger, London, 1988), Chap. 18, p. 324.
[14]G. J. Kearley and J. Tomkinson, Inst. Phys. Conf. Ser. **107**, 245 (1990).
[15]P. Gans, *Vibrating Molecules* (Chapman and Hall, London, 1971).
[16]S. M. Bennington (private communication).
[17]P. J. R. Honeybone, R. J. Newport, W. S. Howells, J. Tomkinson and P. J. Revell, Chem. Phys. Lett. **180**, 145 (1991).
[18]B. Dischler, A. Bubenzer, and P. Koidl, Appl. Phys. Lett. **38**, 1 (1989).
[19]M. Yoshikawa, G. Katagiri, H. Ishida, A. Ishitani, and T. Akamatsu, Solid State Commun. **66**, 1177 (1988).
[20]M. A. Petrich, Mater. Sci. Forum **52**, 377 (1989).
[21]M. Cardona, Phys. Status Solidi B **118**, 463 (1983).
[22]F. R. Dollish, W. G. Fately, and F. F. Bentley, *Characteristic Raman Frequencies* (Wiley, New York, 1974).
[23]G. Herzberg, *Molecular Spectra and Molecular Structure I - Spectra of Diatomic Molecules* (Van Nostrand, New York, 1950).
[24]B. Dischler (private communication).
[25]P. Koidl, Ch. Wild, B. Dischler, J. Wagner, and M. Ramsteiner, Mater. Sci. Forum **52&53**, 41 (1989).
[26]J. Robertson, Phys. Rev. Lett. **68**, 220 (1992).
[27]M. A. Tamor and K. C. Hass, J. Mater. Res. **5**, 2273 (1990).
[28]J. Robertson, Adv. Phys. **35**, 317 (1986).
[29]J. Robertson, in *Diamond and Diamondlike Films and Coatings,* edited by J. C. Angus, R. E. Clausing, L. L. Horton, and P. Koidl (Plenum, New York, 1991), p. 331.
[30]D. R. McKenzie, D. Muller, B. A. Pailthorpe, Z. H. Wang, E. Kravtchinskaia, D. Segal, P. B. Lukins, P. D. Swift, P. J. Martin, G. Amaratunga, P. H. Gaskell, and A. Saeed, Diamond Relat. Mater. **1**, 51 (1991).
[31]Y. J. Chabal and C. K. N. Patel, Phys. Rev. Lett. **53**, 210 (1984).
[32]P. J. R. Honeybone, R. J. Newport, W. S. Howells, S. M. Bennington, and P. J. Revell, Physica B **180&181**, 787 (1991).